

## Activated Carbon Prepared from Coconut Shell Powder with Low Activation Time as Supercapacitor Electrodes

Memoria Rosi<sup>1\*</sup>, M. Nanang Ziad Fatmizal<sup>2</sup>, Dedy Hendra Siburian<sup>3</sup>, Abrar Ismardi<sup>4</sup>

<sup>1,2,3,4</sup> Engineering Physics Department, School of Electrical Engineering, Telkom University, Indonesia

Corresponding Authors E-mail: [memoriarosi@telkomuniversity.ac.id](mailto:memoriarosi@telkomuniversity.ac.id)

---

### Article Info

#### Article info:

Received: 06-12-2022

Revised: 06-01-2023

Accepted: 08-01-2023

#### Keywords:

Activated carbon; Coconut Shell; Activation time; Supercapacitor; Electrodes

#### How To Cite:

Memoria Rosi, M. N. Z. Fatmizal, Dedy H. Siburian, Abrar Ismardi. Activated Carbon Prepared from Coconut Shell Powder with Low Activation Time as Supercapacitor Electrodes. *Indonesian Physical Review*, vol. 6, no. 1, p 85-94, 2023.

#### DOI:

<https://doi.org/10.29303/ipr.v6i1.205>

### Abstract

In this study, we prepared activated carbon from coconut shell with a low activating time for activated carbon (AC). The coconut shell powder ( $< 100 \mu\text{m}$ ) allows for an effective pyrolysis process and low activation time (30 min) that reduces the cost of production. The AC has characteristics of micropore with average size of 1.9 nm and a surface area of  $460.50 \text{ m}^2/\text{g}$ . For supercapacitor electrode, the AC electrodes have capacitance of 50, 66, and  $67.5 \text{ F/g}$  when 0.5 M, 1 M, and 2 M of  $\text{Na}_2\text{SO}_4$  electrolyte was being inserted, respectively. In addition, the equivalent series resistance (ESR) of the AC electrode was 6.6; 4.3, and  $4.1 \Omega$  for 0.5 M, 1 M and 2 M of  $\text{Na}_2\text{SO}_4$  electrolyte. These results indicate that the coconut shell powder can be an alternative source for supercapacitor application with moderate performance.

Copyright © 2023 Authors. All rights reserved.

### Introduction

Activated carbon (AC) has been used for supercapacitor electrode due to superior surface area, structural stability, and moderate price [1-3]. The common AC has been prepared using pyrolysis method under nitrogen atmosphere in separate stages of carbonization and activation process. The carbonization is usually carried out at more than  $400^\circ\text{C}$ , while the activation temperature is about  $700 - 900^\circ\text{C}$  for 1-3 h [4-6]. The activation was carried out physically and chemically. Physical activation usually occurs by gasification of  $\text{CO}_2$  gas whereas the chemical activation utilizes the activating agent of acid ( $\text{H}_3\text{PO}_4$ ), base ( $\text{NaOH}$ ,  $\text{KOH}$ ) or neutral ( $\text{ZnCl}_2$ ) [7-8]. Literature reports the  $\text{KOH}$  is the most powerful chemical to

create superior surface area and porous structure [9]. Previous study reported that wood, coconut shell, and many other agricultural by-products are potential source of AC [9, 10-12]. Coconut shell has been preferred due to its high carbon content and low ash [13]. To produce AC, the coconut shell is commonly crushed with moderate size of 1-5 mm. The resulted AC has a typical micropore size [14-15].

Supercapacitor is one of the progressive energy storages with interesting performance of rapid charging/ discharging, high power density and long cycle life [1-3]. The potential application of supercapacitor has been explored in Uninterruptible Power Supplies (UPS), hybrid energy storage, power electronics, etc. [1-2, 17]. Supercapacitor, also known as Electric Double-Layer Capacitor (EDLC), exhibited superior capacitance because of the high surface area of the electrode and good ionic transport of the electrolyte [1-3]. For porous electrode, the specific area should be supported by well distributed micropores and mesopore [18]. On the other hand, ionic transport is determined by electrolyte concentration. If the ionic concentration is too low, there will be lack of charge carriers. If the electrolyte concentration is too high, the ionic transport will diminish due to the low water hydration [19]. Therefore, it is important to observe optimal electrolyte concentration to obtain high specific capacitance.

In this study, AC was synthesized from coconut shell powder with a small size of about 100  $\mu\text{m}$  and low activation time of 30 min. The utilize of a small size of coconut shell aims to effectively reduce the heating process whereas the low activation time was to efficiently reduce the cost production. The small size of coconut shell is believed to be effective in the heating process (carbonization and activation). Also, it helps the activating agent (KOH) to intercalate the carbon and produce good porosity. This study elaborates some important aspects related to the supercapacitor electrodes, such as coconut shell size, time activation, and various electrolyte concentration of  $\text{Na}_2\text{SO}_4$ .

## **Experimental Method**

### **Activated carbon preparation and characterization**

The coconut shell powder, obtained from Bandung, Indonesia, was crushed within a size of 100  $\mu\text{m}$ . The coconut shell powder was tested using proximate analysis including carbon value, moisture level, ash content and volatile substance. The chemical analysis of the coconut shell also evaluated in terms of lignin, cellulose, and hemicellulose.

The coconut shell powder was carbonized using a homemade furnace of 500°C to produce the carbon. The produced carbon was immersed in KOH with composition of carbon: KOH of 1:3 (according to the mass ratio). The carbon/KOH mixture was heated at 800°C for 30 min to produce the AC. Finally, the AC was carefully washed with 2 M of HCl and DI water alternately to release the salt residue. The schematic diagram of the AC synthesis is represented in Figure 1.

The textural porosity of the AC was evaluated using Nitrogen Physisorption (Quantachrome Autosorb Automated Gas Sorption). From the Nitrogen Isotherm Physisorption data, the specific surface area can be estimated using Brunauer-Emmett-Teller (BET) technique. The amount of adsorbed nitrogen (total pore volume) is defined at  $P/P_0$  of about 0.99 [20]. The average pore size can be predicted using Barrett, Joyner, and Halenda (BJH) technique [21].

## Electrode Manufacture and Characterization

Supercapacitor electrodes were manufactured from a proper combination of AC, carbon black (CB) as conductive filler (purchase from Graphene Supermarket) and polytetrafluoroethylene (PTFE) as binder (imported from China) with weight composition of 8:1:1. First, the PTFE (1 wt %) was dispersed in N-Methyl-2-pyrrolidone (NMP). Subsequently, the AC and CB were put in by continuously stirring at 40°C until the mixture is completed to be ink. The ink was deposited on stainless steel plate with an area of 1 cm<sup>2</sup> and thickness of 0.25 mm. The stainless steel was previously covered by carbon glue to provide good adhesion of the ink to the plate.

The supercapacitor electrodes were investigated using Corrtest CS310H with various electrochemical methods including of Cyclic Voltammetry (CV), Electrical Impedance Spectroscopy (EIS) and Galvanostatic Charge-Discharge (GCD). The set up measurements were using three electrodes by employing the Platinum plate as a counter electrode, AC electrode as a working electrode, and Ag/AgCl as a reference electrode. The CV was adjusted with speed rate of 10 mV/s. The GCD utilized an applied current of 0.5 mA. The EIS was observed in a frequency scale of 0.1 Hz - 1 kHz. The specific capacitance of the AC electrode can be computed using formulations from CV and GCD data [22]. The EIS data were fitted using a software EIS spectrum analyser to obtain the equivalent series resistance (ESR) [23].

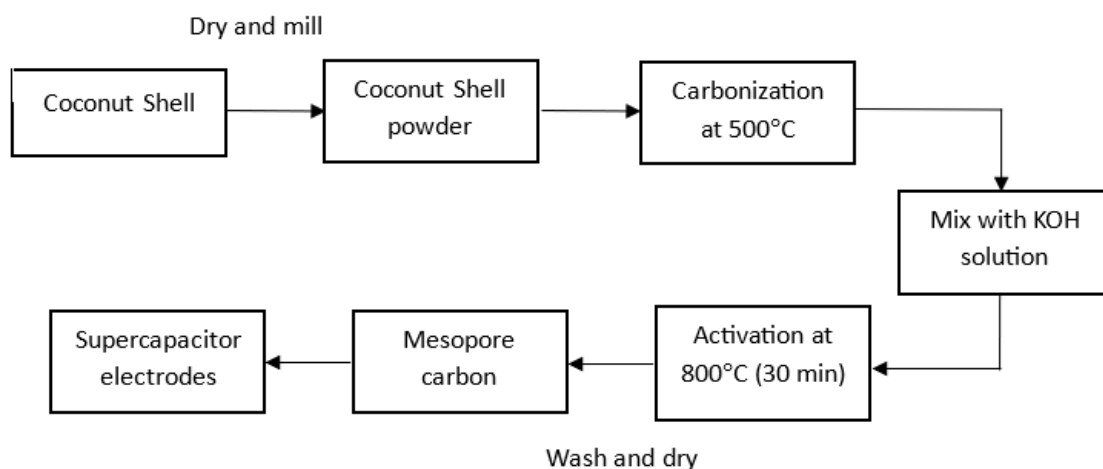


**Figure 1.** The schematic diagram of the AC preparation from coconut shell for supercapacitor electrodes

## Result and Discussion

Figure 2 shows the nitrogen physisorption curve of the nitrogen adsorption/desorption of the AC. The relative pressure of x-axis is a ratio of the adsorptive pressure to the saturated vapor pressure of nitrogen liquid. Along with the measurement, the adsorptive pressure is increased to allow the nitrogen uptake in the volumetric system. The maximum nitrogen level that can be adsorbed into the AC was 290 cc/g. The higher the adsorbed nitrogen, the larger the surface area of the AC [24]. The curve represents a combination of micropores of type I isotherm and small hysteresis loop of H3 which corresponds to mesopore [25-26]. The textural porosity is summarized in Table 3. The total pore volume was 0.45 cc/g and the specific surface area was 460.50 m<sup>2</sup>/g. The BET surface area and pore volume of the AC are still limited compared to

those found elsewhere (9,11-12). These phenomena might come from the excessive amount of KOH inserted in the carbon. The BJH pore size distribution of the AC was demonstrated in the inset picture. The sharp peak curves represent the dominant pores as an average pore size. The moderate pore size of 1.9 nm (table 3) is more convenient for ions accessible in supercapacitor applications. According to our result, we believe that the small size of coconut shell (powder) is responsible for helping the effective activation process to produce micropore and mesopore.

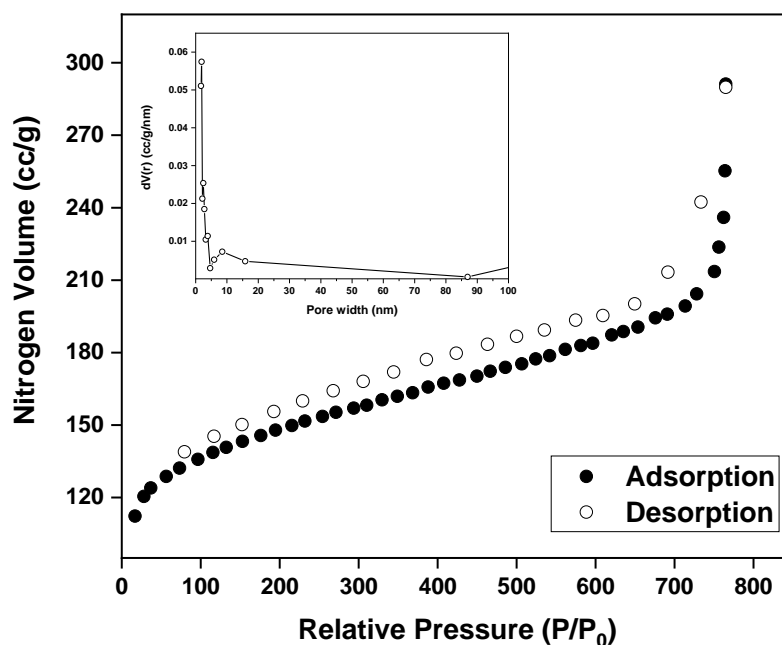
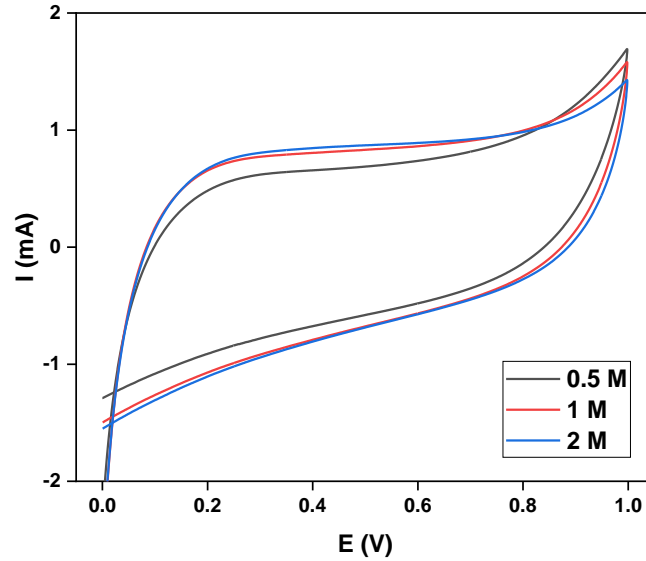


**Figure 2.** Nitrogen physisorption of the AC. Inset picture: BJH pore size distribution of the AC

**Table 1.** The textural porosity of the AC

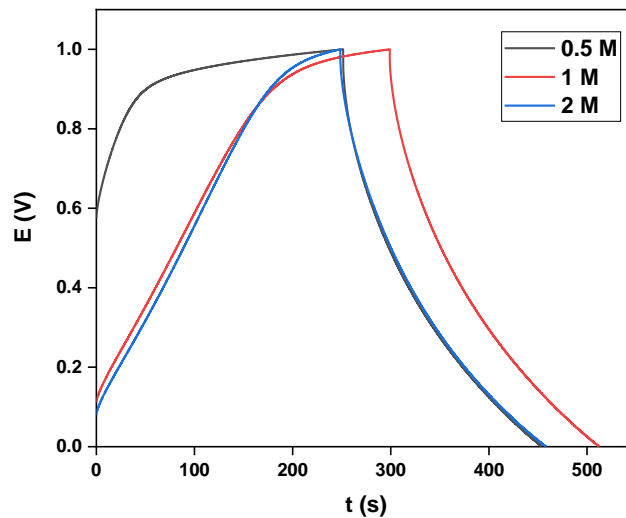
Parameter	Value	Method
Specific area	460.50 m <sup>2</sup> /g	BET
Pore volume	0.45 cc/g	At P/P <sub>0</sub> = 0.99
Pore size	1.9 nm	BJH

Figure 3 shows the CV curve of the AC with various electrolyte content of 0.5 - 2 M. The CV curve has a typical double layer of AC electrode with rectangular-like curve [10]. The CV curve of 0.5 M electrolyte concentration has the smallest area compared to the other. The curve area is proportional to the capacitance [27]. The measured specific capacitance is concise in table 4. The AC with 2 M Na<sub>2</sub>SO<sub>4</sub> has the maximum specific capacitance of 67.5 F/g. The AC with 1 M and 0.5 M Na<sub>2</sub>SO<sub>4</sub> have specific capacitance of 66 and 50 F/g, respectively.



**Figure 3.** CV curve of the AC with various electrolyte concentration 0.5M, 1M, and 2M of  $\text{Na}_2\text{SO}_4$

The GCD curve of the AC with various electrolyte concentration was demonstrated in Figure 4. The AC with electrolyte concentration of 0.5 M and 1 M have the same charging time of 250.50 s but the AC with 1 M has a longer charging time of 298.70 s. The relationship of electrolyte concentration to the charging time is not linear. This result is not clear yet. The discharging time of the electrolyte of 0.5 M, 1 M and 2 M were 201.81, 208.54 and 283.81 s. The higher the electrolyte concentration, the longer the discharging time.



**Figure 4.** GCD curve of the AC with various electrolyte concentration 0.5M, 1M, and 2M of  $\text{Na}_2\text{SO}_4$

Figure 5 shows the EIS curve of the AC with different electrolyte concentrations. All the curves have small semicircles corresponding to high frequency value. The low frequency show the

relatively straight line which analogue to the capacitor performance. The intersection of the semicircle to the Z axis represent the ESR and the straight line related to the capacitive behavior [23]. The AC with electrolyte concentration of 0.5 M has the largest internal resistance of 6.6  $\Omega$ . The electrolyte of 1 M and 2 M has ESR of 4.3 and 4.1  $\Omega$ , respectively.

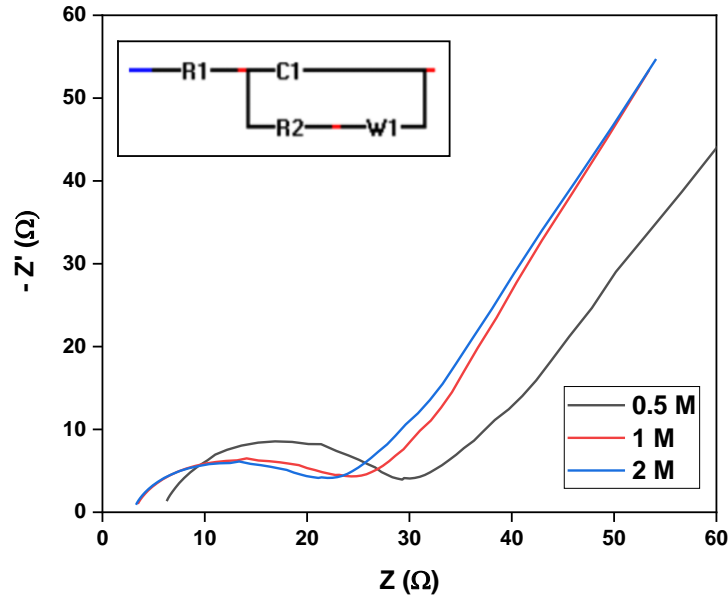


**Figure 5.** EIS curve of the AC with various electrolyte concentration 0.5M, 1M, and 2M of Na<sub>2</sub>SO<sub>4</sub>. Inset picture: electrical circuit analogue of the EIS curve.

**Table 2.** The specific capacitance and ESR of the supercapacitor electrodes

Electrolyte concentration (M)	Specific Capacitance (F/g)	ESR ( $\Omega$ )
0.5	50	6.6
1	66	4.3
2	67.5	4.1

The relationship of different electrolyte concentration to the electrochemical properties of supercapacitor electrodes is explained in Figure 6. It can be concluded that the greater the concentration of Na<sub>2</sub>SO<sub>4</sub>, the superior the specific capacitance is. Also, the greater the electrolyte concentration is, the resulting ESR will be reduced.

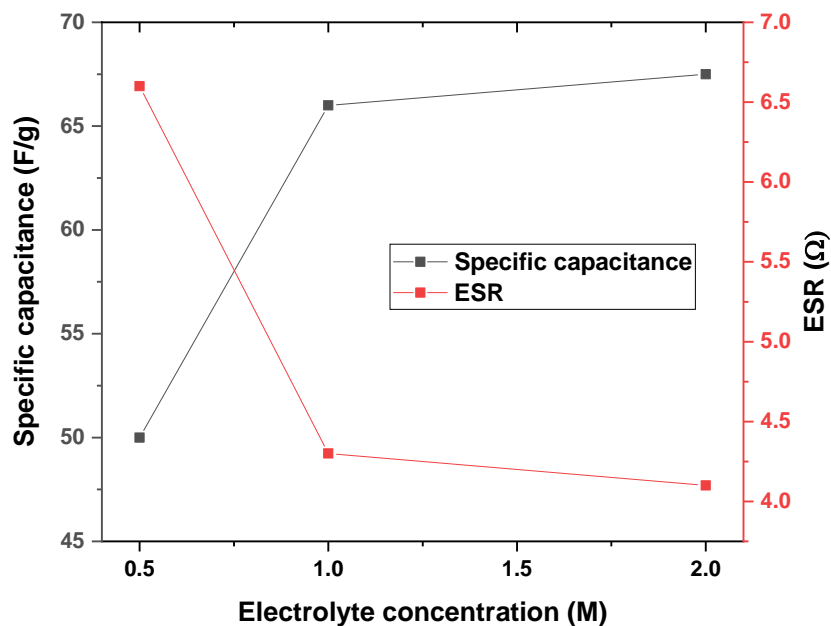


**Figure 6.** Effect of various electrolyte concentration and electrochemical properties of the supercapacitor electrodes

### Conclusion

The AC has been synthesized from the small size of the coconut shell with low activation time. This study demonstrated the formation of micropores and mesopore which contribute to the relatively high surface area. The as-synthesized AC has the potential to be an alternative material for supercapacitors with high capacitance and low internal resistance.

### Acknowledgment

Authors gratefully acknowledge to Telkom University for supporting this Internal Funding “Pendampingan Pendanaan Penelitian BRIN 2020”. The authors thank Labotopia for Nitrogen Physisorption Characterization. In addition, the authors thank the NRE Lab for integrated CV, GCD and EIS characterizations.

### References

- [1] Poonam, K. Sharma, A. Arora, and S.K. Tripathi, “Review of supercapacitors: materials and devices,” *J Energy Storage*, vol. 21, p. 801-825, 2019, doi.org/10.1016/j.est.2019.01.010.
- [2] A. González, E. Goikolea, J.A. Barrena, and R. Mysyk, “Review on supercapacitors: technologies and materials,” *Renewable and Sustainable Energy Reviews*, vol. 58, p. 1189-1206, 2016, doi.org/10.1016/j.rser.2015.12.249.
- [3] Z.S. Iro, C. Subramani, and S.S Dash, “A Brief Review on Electrode Materials for Supercapacitor,” *Int. J. Electrochem. Sci.*, vol. 11, p. 10628-10643, 2016, doi: 10.20964/2016.12.50.

- [4] J. Yin, W. Zhang, N.A. Alhebshi, N. Salah, and H.N. Alshareef, "Synthesis strategies of porous carbon for supercapacitor application," *Small Methods*, vol. 4, no. 3, 1900853, 2020, doi.org/10.1002/smt.201900853.
- [5] S. Ghosh, R. Santhosh, S. Jeniffer, V. Raghavan, G. Jacob, K. Nanaji, P. Kollu, S.K. Jeong, and A.N. Grace, "Natural biomass derived hard carbon and activated carbons as electrochemical supercapacitor electrodes," *Scientific Reports*, vol. 9, no. 16315, 2019, doi.org/10.1038/s41598-019-52006-x.
- [6] P. González-García, "Activated carbon from lignocellulosics precursors: A review of the synthesis methods, characterization techniques and applications," *Renew. Sustain. Energy Rev.*, vol. 82, p. 1393-1414, 2018, doi.org/10.1016/j.rser.2017.04.117.
- [7] J. Zhou, A. Luo, and Y. Zhao, "Preparation and characterization of activated carbon from waste tea by physical activation using steam," *Journal of Air & Waste Management Association*, vol. 68, no. 12, p. 1269-1277, 2018, doi.org/10.1080/10962247.2018.1460282.
- [8] M. Ramón-Gonçalves, L. Alcaraz, S. Pérez-Ferreras, M.E. León-González, N. Rosales-Conrado, and F.A. López, "Extraction of polyphenols and synthesis of new activated carbon from spent coffee grounds," *Scientific Reports*, vol. 9, no. 17706, 2019, doi.org/10.1038/s41598-019-54205-y.
- [9] H. Lu, and X.S. Zhao, "Biomass-derived carbon electrode materials for supercapacitors," *Sustainable Energy Fuels*, vol. 1, issue 6, p. 1265-1281, 2017, doi.org/10.1039/C7SE00099E.
- [10] J. Phiri, J. Dou, T. Vuorinen, P.A.C. Gane, and T.C. Maloney, "Highly porous willow wood-derived activated carbon for high performance supercapacitor electrodes," *ACS Omega*, vol. 4, p. 18108-18117, 2019, doi: 10.1021/acsomega.9b01977.
- [11] T.K. Enock, C.K. King'andu, A. Pogrebnoi, and Y.A.C. Jande, "Status of biomass derived carbon materials for supercapacitor application," *International Journal of Electrochemistry*, 6453420, 2017, doi.org/10.1155/2017/6453420.
- [12] A.M. Abioye and F.N. Ani, "Recent development in the production of activated carbon electrodes from agricultural waste biomass for supercapacitors: A review," *Renew. Sustain. Energy Rev.*, vol. 52, p. 1282-1293, 2015, doi.org/10.1016/j.rser.2015.07.129
- [13] D. Das, D.P. Samal, and B.C. Meikap, "Preparation of activated carbon from green coconut shell and its characterization," *J. Chem. Eng Process Technol*, vol. 6, Issue 5, 1000248, 2015, doi: 10.4172/2157-7048.1000248.
- [14] S.M. Omokafe, A.A. Adeniyi, E.O. Igbafen, S.R. Oke, and P.A. Olubambi, "Fabrication of Activated Carbon from Coconut Shells and its Electrochemical Properties for Supercapacitors," *Int. J. Electrochem. Sci.*, vol. 15, p. 10854-10865, 2020, doi: 10.20964/2020.11.10.

- [15] M. Juan, X.R. Wang, R.J. Fan, W.H. Qu, and W.C. Li, "Coconut-Shell-Based Porous Carbons with a Tunable Micro/Mesopore Ratio for High-Performance Supercapacitors," *Energy Fuels*, vol. 26, no. 26, 5321–5329, 2012, doi.org/10.1021/ef3009234.
- [16] M. Juan, X.R. Wang, R.J. Fan, W.H. Qu, and W.C. Li, "Coconut-Shell-Based Porous Carbons with a Tunable Micro/Mesopore Ratio for High-Performance Supercapacitors," *Energy Fuels*, vol. 26, no. 26, 5321–5329, 2012, doi.org/10.1021/ef3009234.
- [17] L. Zhang, X. Hu, Z. Wang, F. Sun, and D.G. Dorrell, "A review of supercapacitor modeling, estimation, and applications: A control/management perspective," *Renew. Sustain. Energy Rev.*," vol. 81, 2018, dx.doi.org/10.1016/j.rser.2017.05.283.
- [18] J. Yang, H. Wu, M. Zhu, W. Ren, Y. Lin, H. Chen, and F. Pan, "Optimized mesopores enabling enhanced rate performance in novel ultrahigh surface area meso-/microporous carbon for supercapacitors," *Nano Energy*, vol. 33, p. 453-461, 2017, doi.org/10.1016/j.nanoen.2017.02.007.
- [19] S.I. Wong, H. Lin, J. Sunarso, B.T. Wong, and B. Jia, "Optimization of ionic-liquid based electrolyte concentration for high-energy density graphene supercapacitors," *Appl. Mater. Today*, vol. 18, 100522, 2022, doi.org/10.1016/j.apmt.2019.100522.
- [20] J. Bedia, V.M. Monsalvo, J.J. Rodriguez, and A.F. Mohedano, "Iron catalysts by chemical activation of sewage sludge with FeCl<sub>3</sub> for CWPO," *Chem. Engineer J*, vol. 318, p. 224-230, 2017, doi.org/10.1016/j.cej.2016.06.096.
- [21] S. Roldán, I. Villar, V. Ruiz, C. Blanco, M. Granda, R. Menéndez, and R. Santamaría, "Comparison between electrochemical capacitors based on NaOH- and KOH activated carbons," *Energy Fuels*, vol. 24, no. 6 p. 3422–3428, 2010, doi.org/10.1021/ef901538m.
- [22] C. Li, W. Wu, P. Wang, W. Zhou, J. Wang, Y. Chen, L. Fu, Y. Zhu, Y. Wu, and W. Huang, "Fabricating an aqueous symmetric supercapacitor with a stable high working voltage of 2 V by using an alkaline-acidic electrolyte," *Advanced Science*, vol. 6, Issue 1, 1801665, 2019, doi.org/10.1002/advs.201801665.
- [23] M. Sivachidambaram, J.J. Vijaya, K. Niketha, L.J. Kennedy, E. Elanthamilan, and J.P. Merlin, "Electrochemical studies on tamarindus indica fruit shell bio-waste derived nanoporous activated carbons for supercapacitor application," *J Nanosci Nanotechnol.*, vol. 19, no. 6, p. 3388-3397, 2019, doi: 10.1166/jnn.2019.16115.
- [24] K.S.W. Sing, "Physisorption of nitrogen by porous materials," *Journal of Porous Materials*, vol. 2, p. 5-8, 1995, https://doi.org/10.1007/BF00486564.
- [24] X. Song, X. Ma, Y. Li, L. Ding, and R. Jiang, "Tea waste derived microporous active carbon with enhanced double-layer supercapacitor behaviors," *Appl. Surf. Sci.*, vol. 487, p. 189-197, 2019, doi.org/10.1016/j.apsusc.2019.04.277.
- [24] Z. Xu, Z. Yuan, D. Zhang, W. Chen, Y. Huang, T. Zhang, D. Tian, H. Deng, Y. Zhou, and Z. sun, "Highly mesoporous activated carbon synthesized by pyrolysis of waste polyester textiles and MgCl<sub>2</sub>: Physiochemical characteristics and pore-forming mechanism," *J. Clean. Prod.*, vol. 192, p. 453-461, 2018, doi.org/10.1016/j.jclepro.2018.05.007.
- [25] Z. Xu, Z. Yuan, D. Zhang, W. Chen, Y. Huang, T. Zhang, D. Tian, H. Deng, Y. Zhou, and Z. sun, "Highly mesoporous activated carbon synthesized by pyrolysis of waste polyester

- textiles and MgCl<sub>2</sub>: Physiochemical characteristics and pore-forming mechanism," *J. Clean. Prod.*, vol. 192, p. 453-461, 2018, doi.org/10.1016/j.jclepro.2018.05.007.
- [26]L. Su, Q. Zhang, Y. Wang, J. Meng, Y. Xu, L. Liu, and X. Yan, "Achieving a 2.7 V aqueous hybrid supercapacitor by the pH-regulation of electrolyte, *J. Mater. Chem. A.*, vol. 8, issue 17, p. 8648-8660, 2020, doi.org/10.1039/D0TA02926B.